This is the author's version of an article that has been published in the Proceedings of the
IEEE International Conference on Advanced Intelligent Mechatronics (AIM), Banff, AB, July 12-15, 2016, pp. 1297-1304.
The final version of record is available at https://doi.org/10.1109/AIM.2016.7576949

Robust Trajectory Tracking Control for an Ultra Lightweight Tendon Driven Series Elastic Robot Arm

Jérôme Kirchhoff and Oskar von Stryk

***Abstract*— Trajectory tracking control for a tendon driven series elastically actuated robotic arm is considered. This bio-inspired actuation concept enables an ultra lightweight and highly safe robot design that is very well suited for physical human-robot interaction. However, the high elasticity in the joint actuation imposes challenges on robot control, especially for the usual case that no joint torque measurements are available. In this paper, a trajectory tracking controller for this highly compliant robot is presented which does not need explicit joint torque measurements as required by related approaches for robots with elastic joints. A control concept is proposed which aims to be robust against inaccuracies in various model parameters (like robot dynamics, position initialization, drive train stiffness, transmission ratio and friction). It compensates for changes in robot dynamics by equilibrium controlled stiffness. The proposed controller is successfully applied and evaluated in simulated and physical experiments with the robot.**

I. INTRODUCTION

A robotic co-worker can potentially be employed for a number of tasks that are not yet or only partly automated in an industrial environment. Such tasks consist of working steps where the human abilities are needed for repetitive or supporting steps which are difficult to automate efficiently with conventional robotic technology. Also the free space for an additional robotic co-worker is limited. Especially in small and medium enterprises, e.g. with low volume production, such tasks often change, with the result that the robot has to be easily and effectively reprogrammable by a non-expert. Most importantly, the robots must be able to cooperate safely with their human workmate.

Applications with high safety requirements for humans, sharing workspaces with robots, have much different challenges than in conventional automation. This leads to a host of common design decisions for robotic systems intended for safe human-robot interaction. For example a lightweight mechanical structure, a dimension similar to the size of the human arm, or joints that are equipped with force torque sensors to enable e.g. programming by demonstration, or to react on collisions.

The introduction of tendons in a robotic system enables reducing the robot's effective mass by moving the motors closer to the base. As shown in [1] for blunt impacts, it is generally not possible to reduce the collision forces caused by the effective mass by control, because the actuator's time constant is higher than the duration of the first collision force peak. Thus, designing a lightweight robot with a low effective mass is an effective possibility to reduce collision forces and increase safety for humans, if no excessive cushioning of the robot arm structure is desired.

Besides the robot's structure, the reflected inertia of geared motors with high reduction ratios also significantly increases the effective robot arm inertia. Even small elasticities e.g. by using springs in the drive train, dynamically decouple the geared motor from the link inertia and act as a mechanical low pass filter of force peaks, thus protects the robot's structure, gears, tendons and mitigates the severity of the impact.

Control of an elastic tendon driven, ultra lightweight robot poses some special challenges. The lightweight design limits the number of additional sensors used to sense the robot's internal state. Gripping heavy objects, in comparison to the robot's own weight, drastically changes the dynamics and the acting friction forces. If the motor position sensors are relative, their zero position can vary after each initialization. Tasks with contacts, where elastic robots are well suited for, have to be regarded to protect the robot's structure and tendons.

The novel control approach presented in this paper considers the special needs of ultra lightweight elastic tendon driven robots, equipped with motor and joint position sensors. As mentioned in [2] an accurate joint torque value is crucial for controller performance, and it's estimation using only position information leads to unsatisfactory results in presence of model or position errors. Highly accurate robot dynamic models for ultra lightweight tendon driven series elastic arms are difficult to obtain and maintain. Therefore, control approaches are desirable which are robust against changes in model and parameters. This paper introduces a control approach that is suitable for trajectory tracking, robust against model inaccuracies in the drive train, robot dynamics and offsets in position sensing. Furthermore it includes a control torque limitation mechanism to realize safe interaction with the environment.

In more detail, the proposed controller

- contains state feedback with few model dependencies,
- integrates a friction observer [3] in order that it can be used without explicit joint torque measurements,
- is robust against inaccurate initialization of the relative motor sensors, elastic transmission ratios and stiffness coefficients,
- compensates for changes in robot dynamics by equilibrium controlled stiffness,
- contains a contact mode based on an external torque observer [4], [5] without explicit measurement of the joint torques, to enable contact tasks.

The authors are with the Simulation, Optimization and Robotics Group, Department of Computer Science, Technische Universität Darmstadt, Germany [kirchhoff,stryk]@sim.tu-darmstadt.de

Copyright (c) 2016 IEEE. Personal use of this material is permitted. Permission from IEEE must be obtained for all other uses, in any current or future media, including reprinting/republishing this material for advertising or promotional purposes, creating new collective works, for resale or redistribution to servers or lists, or reuse of any copyrighted component of this work in other works.

This is the author's version of an article that has been published in the Proceedings of the
IEEE International Conference on Advanced Intelligent Mechatronics (AIM), Banff, AB, July 12-15, 2016, pp. 1297-1304.
The final version of record is available at https://doi.org/10.1109/AIM.2016.7576949

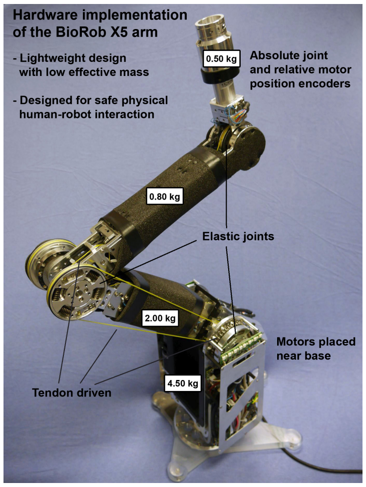

Fig. 1. Hardware implementation of a BioRob X5 arm with four elastically actuated joints (fifth joint not used). The robot arm has a reach of about $75cm$, weights $7.8kg$ including power electronics and has a nominal payload of $500g$. The schematic actuation principle with springs embedded in the joint pulley is depicted in Fig. 2.

The paper is organized as follows. Section II gives a short overview of control strategies for robots with elastic joints. The investigated lightweight elastic robot is introduced in Section III. The components needed to realize trajectory tracking control for this class of robots are described in Section IV and the experimental results are shown in Section V. Finally all key aspects are summarized in Section VI.

II. Related Work

This paper investigates robotic systems with an open serial kinematic chain and highly elastic joints. The joints are driven by electrical actuators using tendons and a series elasticity in the drive train. In contrast to Series Elastic Actuators (SEA) [6], the spring elongation is estimated using the position difference between reflected motor and joint position and is not directly measured.

Control concepts for tendon driven mechanisms with elasticities, actuated in an antagonistic manner have been developed by [7]. Further, [8] developed a control strategy for compliant and noncompliant antagonistic drives based on the biologically inspired puller-follower concept, regarding gravity compensation.

To realize trajectory tracking for robots with elastic joints we first have to investigate which sensor data are provided by the robot. If only the motor positions $\boldsymbol{\theta} \in \mathbb{R}^n$ are measurable, as typically the case for industrial robots, a PD control can be used as presented by [9], with the motor velocities $\dot{\boldsymbol{\theta}} \in \mathbb{R}^n$ estimated by an appropriate filtered numerical differentiation. The desired motor positions $\boldsymbol{\theta_d} \in \mathbb{R}^n$ can be computed with the reduced dynamics model [10] using the desired joint positions $\boldsymbol{q_d} \in \mathbb{R}^n$, it's time derivatives $\dot{\boldsymbol{q}}_{\boldsymbol{d}}$ and $\ddot{\boldsymbol{q}}_{\boldsymbol{d}}$, the diagonal elastic transmission stiffness matrix $\boldsymbol{K} \in \mathbb{R}^{n\times n}$, the mass matrix $\boldsymbol{M} \in \mathbb{R}^{n\times n}$, the matrix $\boldsymbol{C} \in \mathbb{R}^{n\times n}$ of the centrifugal and Coriolis term and the gravity torque vector $\boldsymbol{g} \in \mathbb{R}^n$, as presented in Equation (1) and n being the number of joints.

$$\boldsymbol{\theta}_d = \boldsymbol{q}_d + \boldsymbol{K}^{-1}\left(\boldsymbol{M}(\boldsymbol{q}_d)\ddot{\boldsymbol{q}}_d + \boldsymbol{C}(\boldsymbol{q}_d, \dot{\boldsymbol{q}}_d)\dot{\boldsymbol{q}}_d + \boldsymbol{g}(\boldsymbol{q}_d)\right) \quad (1)$$

The dynamics of an elastic joint, actuated by an electrical motor, can be expressed as four first order differential equations, which determines the length of the corresponding state space vector. If the motor and joint position are measurable, one representation of the state space vector is $(\boldsymbol{\theta}, \dot{\boldsymbol{\theta}}, \boldsymbol{q}, \dot{\boldsymbol{q}})^T$. This definition is beneficial in case each joint and motor is equipped with a position sensor, since the velocities can be derived from the position measurement by numerical differentiation and an appropriate filter.

Feeding back the above robot state enables control strategies like Feedback Linearization [11]. For both, only motor position measurements and additional joint position measurements, one can add a feedforward term to compensate dynamic effects like gravity [12] or the whole dynamics [13].

If direct joint torque sensing is available, the above mentioned state space vector can be replaced by $(\boldsymbol{\theta}, \dot{\boldsymbol{\theta}}, \boldsymbol{\tau}, \dot{\boldsymbol{\tau}})^T$. Control concepts using this information have been developed for robots with flexible joints, e.g., [2], [14], [15] and [16], to realize torque control, impedance control and safe human-robot interaction, producing impressing results.

Joint torque estimation and further model inaccuracies (gravity compensation, spring stiffness, unmodeled tendons), can drastically decrease control performance ([2]) of the mentioned control laws for robots with elastic joints. This motivates the research for a control law that fits to the challenges of tendon driven robots, with flexible joints.

The proposed control concept in this paper can be classified according to [17] as *passive compliant motion* control with *fixed passive compliance*. This classification further can be refined to *passive, equilibrium-controlled stiffness* [18], since the equilibrium position of the springs can be changed by adjusting the desired motor position. This exerts a desired force or stiffness according to the position adjustment which results in a position-control problem instead of a force-control problem.

III. The ultra lightweight BioRob arm with tendon driven SEAs

The BioRob X5 arm [19] is a tendon driven robot with four elastic, rotary joints (see Fig. 1). The tendon is regarded as stiff in comparison to the elastic joints. Elasticity is introduced into the mechanical structure with springs, placed in the joint's pulleys. This is shown in Figure 2 for one single elastic joint. In the following section we summarize and extend the results of [20] for a single joint to realize joint torque estimation for the considered robot.

According to the shown structure, the motor torque τ_m is transferred through the gear box and tendons to the joint. Here, one has to regard two ratios, the gear box ratio n_g and the transmission ratio n_t. The transmission ratio n_t is determined by the radius r of the motor pulley and the radius R of the joint pulley:

$$n_t = \frac{R}{r}$$

Copyright (c) 2016 IEEE. Personal use of this material is permitted. Permission from IEEE must be obtained for all other uses, in any current or future media, including reprinting/republishing this material for advertising or promotional purposes, creating new collective works, for resale or redistribution to servers or lists, or reuse of any copyrighted component of this work in other works.

This is the author's version of an article that has been published in the Proceedings of the
IEEE International Conference on Advanced Intelligent Mechatronics (AIM), Banff, AB, July 12-15, 2016, pp. 1297-1304.
The final version of record is available at https://doi.org/10.1109/AIM.2016.7576949

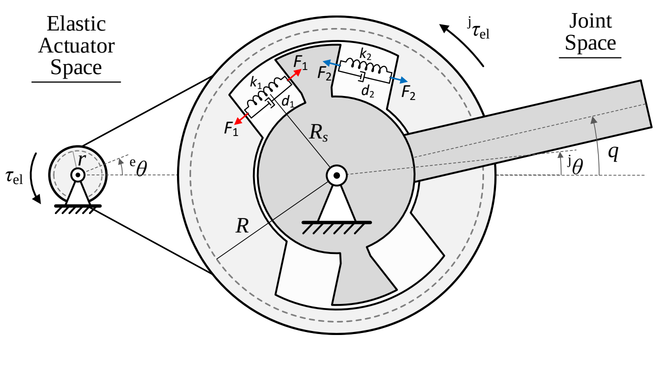

Fig. 2. Model of the elastic transmission adapted from [21]. Springs are placed in pulley. Parameters are: elastic actuator torque τ_{el}, elastic actuator joint torque ${}^{j}\tau_{el}$, spring forces F_i, spring stiffness k_i, spring damping d_i, motor pulley radius r, joint pulley radius R, spring radius R_s, angular joint position q, angular motor position ${}^{e}\theta$ with respect to the elastic actuator and joint ${}^{j}\theta$.

Using these ratios, one can reflect the motor positions into joint space

$$ {}^{e}\theta = \frac{1}{n_g} \cdot \theta \ , \quad {}^{j}\theta = \frac{1}{n_t} \cdot {}^{e}\theta \ . $$

The reflected motor position can now be used to compute the acting joint torque. Since the spring stiffness coefficient is known from the spring's data sheet, we can compute the joint torque by the displacement between the reflected motor position ${}^{j}\theta$ and the joint position q.

Analog to [21], before estimating the elastic joint torque ${}^{j}\tau_{el}$, one has to determine how the reflected motor position and joint position affect the spring displacement x_1 and x_2 of opposing springs.

If the springs are placed in the joint pulley, one first has to regard that the linear spring displacement results from an rotary displacement. Second, the spring force acts at the radius R_s unequal R. With the ratio $\frac{R_s}{R}$ that transforms the linear displacement of $\left(q -^{j} \theta\right)$ at radius R to the springs at radius R_s, the spring elongation can be formulated as

$$ x_2 = -x_1 = R \sin\left(q - {}^{j}\theta\right) \cdot \frac{R_s}{R} = R_s \sin\left(q - {}^{j}\theta\right) . $$

Now we are able to define the force F_i that is exerted by the stretched springs $i \in [1, 2]$ and estimate the elastic joint torques, containing the force $F_{p,i}$ of the prestreched springs, analog to [20] as

$$ F_i = k_i \left(l_{\mathrm{p}_i} + x_i\right) + d_i \, \dot{x}_i \qquad F_{p,i} = k_i \, l_{\mathrm{p}_i} \ , $$

with spring stiffness k_i and prestretching spring displacement l_{p_i}. Assuming that the damping forces are small, compared to the spring elongation and prestretched force:

$$ F_i \approx F_{p,i} + k_i \, x_i \ . $$

This results in a joint torque estimation

$$ \begin{aligned} {}^{j}\tau_{el} &= R_s \left(F_{p,1} + k_1 \, x_1\right) - R_s \left(F_{p,2} + k_2 \, x_2\right) \\ &= -R_s^2 \left(k_1 + k_2\right) \, \sin\left(q - {}^{j}\theta\right) \\ &= -k_e \, \sin\left(q - {}^{j}\theta\right) , \end{aligned} \tag{2} $$

with $F_{p,1} = F_{p,2}$ and joint stiffness

$$ k_e = R_s^2 \left(k_1 + k_2\right) . \tag{3} $$

IV. Trajectory Tracking for Tendon Driven Robots With Elastic Joints

A. Goals

A control design for tendon driven robots with elastic joints is to be developed, which enables trajectory tracking and can handle contact situations. For this purpose, only motor and joint position information are available. The control structure has to be robust against system changes that are not modeled.

The controller's performance is influenced by the accuracy of the modeled system behavior. If the motor position sensors are relative, their position can vary between each initialization. Nevertheless, the trajectory tracking performance should not. Friction forces constitute another crucial performance influence. Especially for lightweight robot arms, high friction forces can drastically increase time to fulfill a planned motion. Additionally, load dependent friction effects are hard to model and to identify. At least if heavy pieces, in comparison to the robots weight, have to be lifted, the model based desired motor position computations result in wrong values.

Contact tasks are of special interest. Beside the possibility to define contact forces in the trajectory, the controller should contain a basic contact behavior. The reason for this is, if contact situations are not regarded, the controller, probably designed with integral component, continuously increases the control torque resulting in damage of the environment or the robot's lightweight structure itself.

For better readability all variables are assumed as reflected to the joint side, omitting the subscription in the rest of this paper.

B. Approach

In the next sections we will introduce a basic state space controller for position control, that constitutes the starting point of our investigations. It is shown that for good performance multiple assumptions are made. These assumptions need to be significantly relaxed in the environment of the investigated tendon driven lightweight robot arm, with joint elasticities.

To improve the controller's robustness against not modeled or changing friction effects, a friction observer is introduced and it is investigated how it can be used if explicit joint torque measurements are not available. This will build one extension component for the aimed state space controller.

Since changes in the robot's rigid body dynamics model have to be regarded, we introduce the method of equilibrium controlled stiffness to include the current robot dynamics into the position control law.

Since the estimated joint torque (2) is used in both, the equilibrium controlled stiffness and the friction observer, the torque limitation is described in the context of the whole controller design.

Copyright (c) 2016 IEEE. Personal use of this material is permitted. Permission from IEEE must be obtained for all other uses, in any current or future media, including reprinting/republishing this material for advertising or promotional purposes, creating new collective works, for resale or redistribution to servers or lists, or reuse of any copyrighted component of this work in other works.

This is the author's version of an article that has been published in the Proceedings of the
IEEE International Conference on Advanced Intelligent Mechatronics (AIM), Banff, AB, July 12-15, 2016, pp. 1297-1304.
The final version of record is available at https://doi.org/10.1109/AIM.2016.7576949

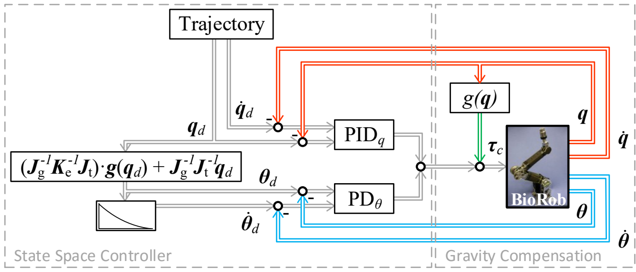

Fig. 3. State space controller with feedback of whole robot state $(\boldsymbol{q}, \dot{\boldsymbol{q}}, \boldsymbol{\theta}, \dot{\boldsymbol{\theta}})^T$, desired motor position θ_d and velocity $\dot{\boldsymbol{\theta}}$ computation, as well as model based gravity compensation producing the control torque $\boldsymbol{\tau}_c$.

C. State Space Controller

One possibility to realize a controller with state feedback, for trajectory tracking is shown in Figure 3. The controller is based on the PD controller by [9] and extended to a full state feedback controller with state vector $(\boldsymbol{q}, \dot{\boldsymbol{q}}, \boldsymbol{\theta}, \dot{\boldsymbol{\theta}})^T$. The desired motor position is computed according to (1), but only using the gravity vector of the desired joint position $\boldsymbol{g}(\boldsymbol{q_d})$, regarding the kinematic joint coupling with the coupling matrix $\boldsymbol{J}_t$ and gearing matrix $\boldsymbol{J}_g$. To get the desired motor velocity, the numerical differences of $\boldsymbol{\theta}_d$ are computed with subsequent low pass filtering. As online gravity compensation, the torques produced by the model based gravity compensation at the current joint position are added to the control torque. To reduce position overshooting at the target point, the integrational term is activated on arrival at a certain Cartesian position accuracy.

The position accuracy of the state space multiple-input multiple-output controller in Figure 3 is limited, because of multiple assumptions that are made:

- All gravity effects can be computed by the gravity torque vector model $\boldsymbol{g}(q)$.
- The joint equilibrium position equals the reflected motor position.
- The elastic tendon transmission is accurately modeled.
- The modeled actuator friction is a close representation of the real friction.
- Aging of the system or gripping of objects does not change any system parameters.

Even if e.g., the gravity effort vector, the elastic transmission, or the friction effects can be modeled, these models are often simplifications of the real system behavior with more or less accurate identified model parameters.

In the control structure in Figure 3, all deviations from the assumptions made, are compensated by the joint side PID controller. Large errors in the model for gravity compensation leads to an over- or undercompensation that has to be compensated by other controller components. Errors in the elastic transmission model (e.g., in joint stiffness k_e) result in deviations for the computed desired motor position θ_d. In this case, the motor side PD controller goal differs from the joint side PID controller. If the modeled friction torques are smaller than the real friction torques, the robot only starts moving if the control signal exceeds the friction torques. Model parameter changes caused by aging effects or gripped objects have to be regarded. Motor position initialization errors lead to deviations between the desired motor position and the actually needed motor position.

All these negative effects on the joint position accuracy can be reduced by increasing the PID controller's proportional and integrational term. The size of the proportional term is limited by system stability. But using a high integrational term during trajectory tracking limits the controller's performance because of possible overshooting at the target point and thus long settling time.

D. Joint Torque Estimation Based Friction Compensation

Elastic joint robots with only motor and joint position measurement, as described above, do not have the possibility to directly measure joint torques. The control approach presented in this paper integrates the friction observer structure developed by [3] for robots with joint torque sensing and adapts it to tendon driven, elastic robotic arms with indirect motor and joint position-based joint torque estimation. The resulting controller structure only needs few model knowledge. This allows to cope with effects that are hard to model and to identify, e.g. load dependent friction effects.

The friction observer is inspired by the momentum-based observer of [4], [5] that estimates the torques produced by external forces acting on the rigid body dynamics. Since only the drive train friction is estimated and the (indirectly measured) elastic joint torque represents the robot arm structure dynamics, only the linear actuator dynamics is regarded in the observer. The actuator dynamics can be described by

$$\tau_m = I_m \ddot{\theta} + \tau_{el} + \tau_f, \tag{4}$$

with motor torque τ_m, motor acceleration $\ddot{\theta}$, motor inertia I_m, elastic joint torque τ_{el} (including visco-elastic effects of the transmission) and friction torque τ_f. Considering (4), the observer dynamics can be described by

$$\tau_m = I_m \ddot{\hat{\theta}} + \tau_{el} + \hat{\tau}_f \tag{5}$$

$$\hat{\tau}_f = -L I_m \left(\dot{\theta} - \dot{\hat{\theta}} \right), \tag{6}$$

with $L > 0$, $\hat{\tau}_f$ friction estimation, $\ddot{\hat{\theta}}$ reflected motor acceleration estimation and $\dot{\hat{\theta}}$ the estimated reflected motor velocity.

Combining (4) with (5) and (6) shows that the friction is effectively estimated using a first order low-pass filter

$$\hat{\tau}_f = \frac{1}{L^{-1}s + 1} \tau_f,$$

where s is the Laplace operator, and $L = 1/T$ the reciprocal of the filter's time constant T. Finally the estimated friction can be compensated, by simply adding $\hat{\tau}_f$ to the control torque τ_c:

$$\tau_m = \tau_c + \hat{\tau}_f. \tag{7}$$

As input, the observer only requires the computed controller torque, the motor velocity and the measured joint torque.

Copyright (c) 2016 IEEE. Personal use of this material is permitted. Permission from IEEE must be obtained for all other uses, in any current or future media, including reprinting/republishing this material for advertising or promotional purposes, creating new collective works, for resale or redistribution to servers or lists, or reuse of any copyrighted component of this work in other works.

This is the author's version of an article that has been published in the Proceedings of the
IEEE International Conference on Advanced Intelligent Mechatronics (AIM), Banff, AB, July 12-15, 2016, pp. 1297-1304.
The final version of record is available at https://doi.org/10.1109/AIM.2016.7576949

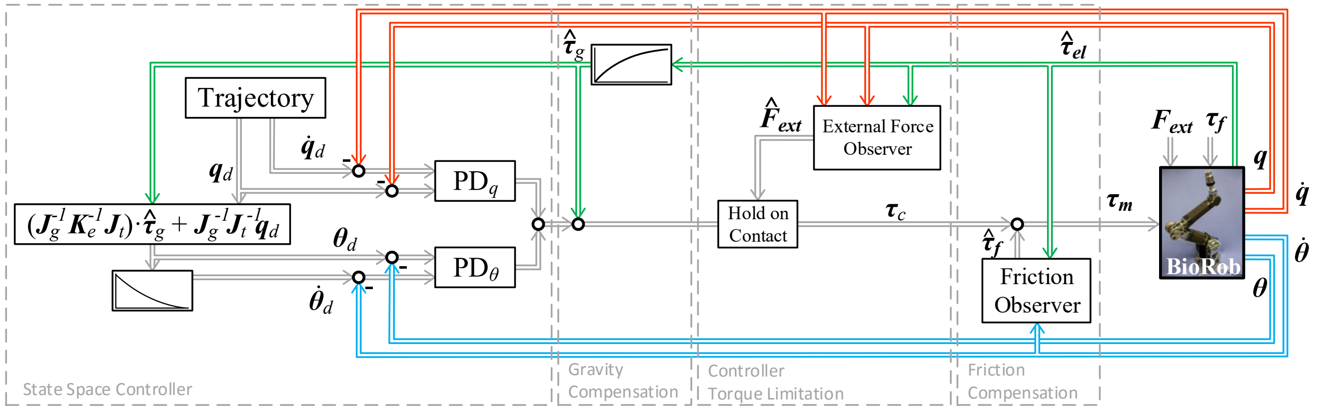

Fig. 4. State space controller extended with friction compensation $\hat{\tau}_f$, torque limitation based on external force estimation $\hat{F}_{ext}$ and feedback of estimated joint torque $\hat{\tau}_{el}$ for gravity compensation and equilibrium controlled stiffness.

Since we cannot measure the needed joint torques, as done in [3], we have to investigate how inaccuracies in the estimated joint torque $\hat{\tau}_{el}$ alter the behavior of the observer. For this purpose, we consider the friction torque estimation after introduction of an error ϵ. This error represents the inaccuracies introduced by the joint torque estimation $\hat{\tau}_{el}$, computed by (2). The friction observer should represent the real actuator dynamics, which leads to the following equation

$$I_m\ddot{\theta} + \tau_{el} + \tau_f = I_m\ddot{\hat{\theta}} + \hat{\tau}_{el} + \hat{\tau}_f$$

Introducing the joint torque estimation error leads to

$$I_m\ddot{\theta} + \tau_{el} + \tau_f = I_m\ddot{\hat{\theta}} + \tau_{el} + \epsilon + \hat{\tau}_f$$
$$\Leftrightarrow I_m\left(\ddot{\theta} - \ddot{\hat{\theta}}\right) = \epsilon + \hat{\tau}_f - \tau_f \tag{8}$$

After transformation into Laplace space and subsequently dividing Eq. (8) by (6), one obtains the filtered friction estimation with

$$\frac{I_m s^2\left(\Theta - \hat{\Theta}\right)}{-LI_m s\left(\Theta - \hat{\Theta}\right)} = \frac{\epsilon + \hat{\tau}_f - \tau_f}{\hat{\tau}_f} \tag{9}$$

$$\Leftrightarrow \hat{\tau}_f = (\tau_f - \epsilon)\,\frac{1}{L^{-1}s + 1} \tag{10}$$

Equation (10) shows that the introduction of ϵ also causes an error in friction torque estimation.

Another observer property concerns its steady state, where the estimated motor acceleration is $\ddot{\hat{\theta}} \overset{!}{=} 0$. So, the observer dynamics (5) becomes

$$0 = \tau_m - \tau_{el} - \hat{\tau}_f.$$

Using the estimated friction $\hat{\tau}_f$ for friction compensation, as proposed in (7), leads to the requirement

$$0 = \tau_c - \tau_{el} \Rightarrow \tau_c \overset{!}{=} \tau_{el}. \tag{11}$$

Since the control torque τ_c is computed using a model based gravity compensation, and τ_{el} estimated according to the transmission model, errors in both models will violate the requirement of Eq. 11. In this case the observer will adjust its friction estimation $\hat{\tau}_f$, and thus τ_m until Eq. (11) holds. Depending on the model errors, this will lead to a friction compensation in Eq. (7) acting against the control torque τ_c resulting in an over- or undercompensation, which leads to static position errors.

The two investigated properties lead to the following conclusions that are of special relevance for tendon driven robots with joint elasticities. Errors in joint torque estimation yield to errors in friction estimation. Further, at steady-state the control torque should equal the estimated joint torque to avoid undesired over or under compensation.

E. Equilibrium Controlled Stiffness

Besides the control errors introduced by insufficient modeled friction, inaccurate elastic transmission ratio, joint stiffness, or motor initialization error, the error in computation of the desired motor position θ_d as done in Eq. (1) negatively influences the control performance. Especially using the inverse dynamics model in desired motor position computation presents special challenges. These arise because the current joint position, velocity and accelerations are needed, the dynamics parameters have to be identified and the gripped object's physical parameters have to be included.

To avoid these difficulties, one can benefit from the joint torque estimates. Feedback of the estimated joint torques into the calculation of the desired motor trajectory (1) cancels out most of the joint torque measurement errors described in Section IV-C. The resulting feedback controller structure is depicted in Figure 4, where feedback of the estimated joint torque is highlighted in green.

F. State Space Controller with Friction Compensation

The final controller structure combines different controller components to achieve robustness against the possible model errors discussed in the previous sections. The control error is reduced by a linear control law containing the motor side PD and joint side PD controller. The next step contains the gravity compensation. Here, the estimated and filtered elastic joint torque is used as compensation value. This enables the usage of the presented friction observer since

Copyright (c) 2016 IEEE. Personal use of this material is permitted. Permission from IEEE must be obtained for all other uses, in any current or future media, including reprinting/republishing this material for advertising or promotional purposes, creating new collective works, for resale or redistribution to servers or lists, or reuse of any copyrighted component of this work in other works.

This is the author's version of an article that has been published in the Proceedings of the
IEEE International Conference on Advanced Intelligent Mechatronics (AIM), Banff, AB, July 12-15, 2016, pp. 1297-1304.
The final version of record is available at https://doi.org/10.1109/AIM.2016.7576949

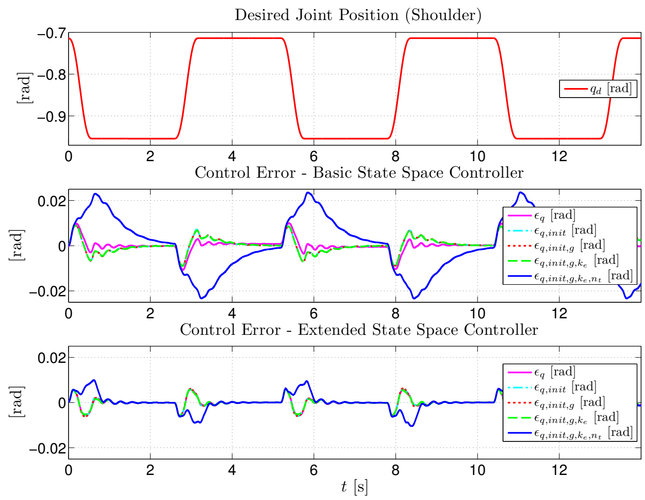

Fig. 5. Desired shoulder trajectory q and the resulting control position error containing the various model inaccuracies for the basic state feedback controller with gravity compensation as well as for the extended state feedback controller with friction compensation, equilibrium controlled stiffness and feedback of the estimated elastic torque, executed in simulation.

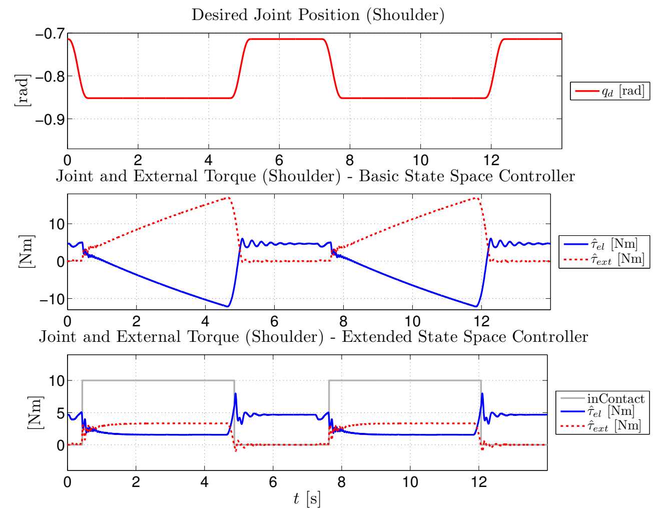

Fig. 6. Comparison of the estimated external joint torques $\hat{\tau}_{ext}$ and elastic joint torques $\hat{\tau}_{el}$ of the basic and extended state space controller, executed in simulation. A "inContact" value of 10 indicates that the controller is in contact mode.

now requirement (11) is met. As described in Section IV-D the friction observer receives the control torque value, the current motor velocity and the estimated elastic joint torque to compute the friction estimation, which is subsequently added to the control torque as friction compensation.

In the case of contacts, feeding back the estimated joint torques to compute the desired motor position, results in an equilibrium controlled stiffness that acts into the contact. Thus, the estimated joint torque, as well as the resulting controller torque will further increase and raise the contact force. To avoid this unwanted behavior, the external force observer [4] that estimates the external end effector force $\hat{F}_{ext}$ and the corresponding external joint torques $\hat{\tau}_{ext}$ is applied. The transition between contact and free controller mode is based on the force $\hat{F}_{ext}$. If it exceeds a tunable threshold, the control torque produced by the state space and gravity compensation parts is kept constant. This alters the behavior of the controller that keeps the contact force constant and thereby protects the robot itself and it's environment.

V. Experimental Evaluation

The presented basic and extended controller designs are evaluated by experiments in simulation and with the robot. First, the controller behavior is investigated in simulation, which offers the ability to change model accuracies and compare both controllers. Furthermore, it is possible to simulate contact situations without damaging a real robot.

The first experiment compares both controllers regarding the influence of different model inaccuracies to the joint control error. During the experiment the robot executes a pick trajectory that simulates gripping of an object with subsequent vertical lifting.

The next experiment investigates the control torque in case of contact. To simulate the contact situation, the same pick trajectory as before is executed but with the lower pick position being placed purposely inside the obstacle (e.g. a table).

The next two experiments are executed on the real BioRob X5 arm. This time the robot has to pick an object. The object changes the robot's physical dynamics parameters and, thus, the model based gravity compensation and the desired motor position computation is no longer accurate for the basic state space controller. The performance of both controllers for tracking the same reference trajectory are compared respecting the Cartesian error to the target position (Euclidean norm), and execution time till the target point is reached.

Finally, the Cartesian accuracy and overall execution time of a benchmark diagonal Inch-Foot-Inch trajectory is investigated. The planned pick trajectory and Inch-Foot-Inch trajectory can be seen in Figure 9.

The controller parameters are tuned for both controllers by experiment based on [22], first for motor side till good performance is reached, then for joint side with subsequently manual tuning to regard the influence of the kinematic coupling of the BioRob X5 arm.

A. Evaluation in Simulation

First a pick motion with $10cm$ vertical lift is executed. To investigate the influence of possible model inaccuracies, we introduce intentionally for both controllers a motor position offset of $2.0°$ simulating an initialization error (including gear backlash), a gravity torque error of 20%, a spring stiffness error of 20% and an elastic transmission ratio error of 20%, marked in Figure 5 with the subscript $init$, g, k_e and n_t respectively. Regarding the basic state space controller (see Figure 5 center plot), all added errors negatively influence the position accuracy. One can observe that the control error slowly diminishes. Especially the elastic transmission ratio model error results in a large control error.

Copyright (c) 2016 IEEE. Personal use of this material is permitted. Permission from IEEE must be obtained for all other uses, in any current or future media, including reprinting/republishing this material for advertising or promotional purposes, creating new collective works, for resale or redistribution to servers or lists, or reuse of any copyrighted component of this work in other works.

This is the author's version of an article that has been published in the Proceedings of the
IEEE International Conference on Advanced Intelligent Mechatronics (AIM), Banff, AB, July 12-15, 2016, pp. 1297-1304.
The final version of record is available at https://doi.org/10.1109/AIM.2016.7576949

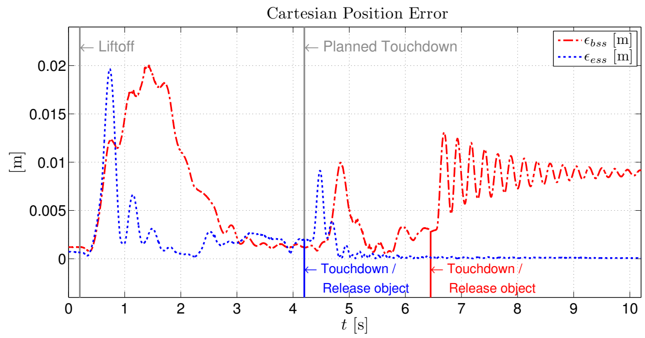

Fig. 7. Comparison of the Cartesian position error and execution time of the basic ϵ_{bss} and extended state space controller ϵ_{ess}, during lifting a object weighting $500g$, executed on the real robot.

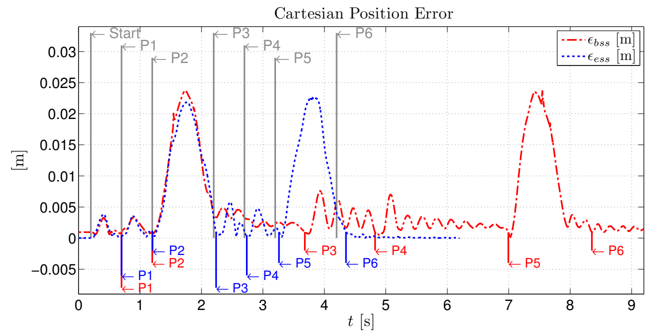

Fig. 8. Comparison of the Cartesian position error and execution time of the basic ϵ_{bss} and extended state space controller ϵ_{ess}, during Inch-Foot-inch trajectory execution on the real robot. Marks *P1-P6* indicate the trajectory point's planned (gray) and executed reaching time.

Considering the extended state space controller, the first three model inaccuracies do not increase the joint position error. Solely the elastic transmission ratio model error increases the control error peak, which is reduced rather immediately, compared to the basic state space controller. In total, the error curves are a bit less oscillating and the control error is removed faster than with the basic state space controller.

The experiment shows that the proposed controller is only sensitive on elastic transmission ratio errors, since the reflected motor position error increases and thus the estimated joint torque. This will be equalized by the friction observer delayed by it's time constant resulting in an overshoot peak.

Repeating the experiments with changing model errors in the ranges $[-20°, 20°]$ initialization error, $[-50\%, 100\%]$ gravity torque error, $[-50\%, 100\%]$ spring stiffness error showed no change of the extended state space control performance. Only the elastic transmission ratio errors again increased the over- or undershoot error which is canceled out with no static control error.

For the pick trajectory with contact, the lower pick point has been placed $1cm$ in the ground (e.g., Table). Figure 6 depicts the estimated external joint torques $\hat{\tau}_{ext}$ from the disturbance observer and the estimated joint torques $\hat{\tau}_{el}$. As expected, the control torque of the basic state space controller continues to increase in contact. In contrast, the new control approach reacts on the estimated external force and keeps the control torque constant during contact. This results in a nearly constant joint torque and thus end effector force.

B. Evaluation in Experiments with the Real Robot

To evaluate the trajectory tracking performance of both controllers by experiment, the Cartesian position error computed from the measured and desired joint angles is investigated. In all experiments the inaccuracies, former artificially introduced in simulation (like initialization error, inaccurate elastic transmission stiffness and ratio, model based gravity compensation and joint torque estimation) are present.

Figure 7 shows the Cartesian position error for a lift task. Here, an object of $500g$ is picked up from the table, vertically lifted about $15cm$ and placed back on the table. The lift and lower motion is planned with a duration of $2s$. The top position has to be reached with an accuracy about $1mm$, the release position with $3mm$ accuracy. The liftoff and planned touchdown time are shown in gray.

The Cartesian errors in Figure 7 show, that the extended state space controller (see. Figure 4) outperforms the basic one. The planned execution time is met (see blue touchdown mark). In contrast to the basic controller, the extended one compensates the dynamics change caused by releasing the object with only a short peak. It rather immediately eliminates the resulting control error.

Similar results can be seen in Figure 8, for the Inch-Foot-Inch trajectory. The trajectory is defined with only stop points that have to be reached with an accuracy of $1mm$. As in the previous experiment, the extended state space controller eliminated the position errors at the stop points rather immediately, and closely met the planned execution times (indicated by the gray marks). In contrast, the basic state space controller needs more time to reduce the position error caused by model inaccuracies, initialization error and unmodeled effects, till the accuracy threshold is reached. Since the trajectory continues as soon as the trajectory points are reached, this results in a longer execution time.

These experiments showed that the presented control approach reaches a good performance in trajectory tracking. The planned execution times are almost met. Feeding back the estimated joint torques $\hat{\tau}_{el}$ does not negatively affect the control performance or cause oscillation effects. It rather enables to consider changes in the robot's rigid dynamics. Even in fast pick motions, where the estimated joint torques are partially influenced by torques of dynamic effects, the performance is only few oscillating.

VI. Conclusion

In this paper, a robust trajectory tracking control approach for tendon driven, ultra lightweight robots with elastic joints has been presented. It does not depend on highly accurate models of robot dynamics or elastic drive train. Furthermore, it only requires the measured angular joint and angular motor position. Explicitly measured joint torques are not available but estimated via the reflected motor and joint position difference and the elastic transmission spring stiffness.

Copyright (c) 2016 IEEE. Personal use of this material is permitted. Permission from IEEE must be obtained for all other uses, in any current or future media, including reprinting/republishing this material for advertising or promotional purposes, creating new collective works, for resale or redistribution to servers or lists, or reuse of any copyrighted component of this work in other works.

This is the author's version of an article that has been published in the Proceedings of the
IEEE International Conference on Advanced Intelligent Mechatronics (AIM), Banff, AB, July 12-15, 2016, pp. 1297-1304.
The final version of record is available at https://doi.org/10.1109/AIM.2016.7576949

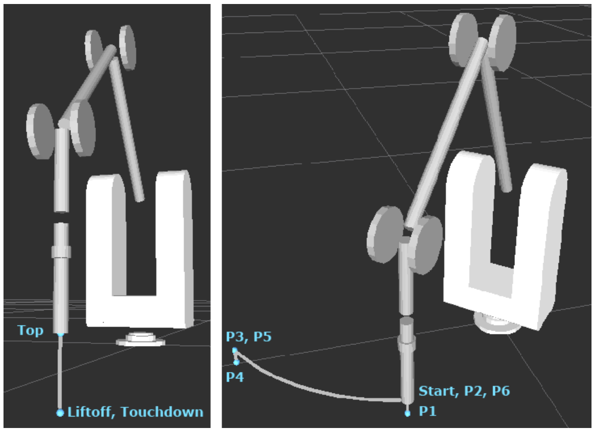

Fig. 9. Visualization of the planned pick and Inch-Foot-Inch trajectory, used for experiments.

The proposed controller adapted two observer strategies, initially developed on robots with joint torque sensing and only moderate joint elasticity. In addition, it uses the estimated joint torques as feedback information for gravity compensation and equilibrium controlled stiffness. This enables to react on changes in the robot's dynamics caused e.g. by gripped objects with not previously known masses.

To cope with contact situations, the controller checks the estimated external end effector force and switches to a contact mode if this force exceeds a user defined threshold. This contact mode holds the control torque till the contact is released again. Thus, in contrast to a PID controller, the produced joint torques do not continue to increase. This protects the robot's structure as well as the environment which may include human workmates.

It has been shown by simulation and experiment that the proposed controller compensates the drawbacks of joint torque estimation and is robust against various model inaccuracies. The used friction compensation in combination with the estimated joint torques of the elastic joints acts like an integrational term, improving control performance in accuracy, settling time and oscillation effects. The equilibrium controlled stiffness scheme further enables compensation against dynamics changes like introduced by gripped obstacles.

To reduce the influence of noise, the used observers and the fed back estimated joint torques are low pass filtered. The tuned time constant influences the reactivity of the controller. This has to be regarded in each specific system.

The introduced approach can also be used if one introduces additional elastic joints in the lower arm (yaw rotation) and at the end effector (roll rotation), equipped with motor and joint position sensors, to create a full 6 DoF robot.

ACKNOWLEDGMENT

This work has been partially supported by the Hessian State Ministry of Higher Education, Research and the Arts (HMWK) under grant 438/14-28.

The authors would like to thank Thomas Lens and Janis Wojtusch for valuable discussions and comments.

REFERENCES

[1] S. Haddadin, A. Albu-Schäffer, and G. Hirzinger, "Safety evaluation of physical human-robot interaction via crash-testing," in *Robotics: Science and Systems*, 2007, pp. 217–224.
[2] A. Albu-Schäffer, C. Ott, and G. Hirzinger, "A unified passivity-based control framework for position, torque and impedance control of flexible joint robots," *Int. J. Robotics Research*, vol. 26, no. 1, pp. 23–39, 2007.
[3] L. Le Tien, A. Albu-Schäffer, A. De Luca, and G. Hirzinger, "Friction observer and compensation for control of robots with joint torque measurement," in *Proc. IEEE/RSJ Int. Conf. Intelligent Robots and Systems*, Sept 2008, pp. 3789–3795.
[4] A. De Luca and R. Mattone, "Actuator failure detection and isolation using generalized momenta," in *Proc. IEEE/RSJ Int. Conf. Intelligent Robots and Systems*, 2003, pp. 634–639.
[5] A. De Luca, A. Albu-Schäffer, S. Haddadin, and G. Hirzinger, "Collision detection and safe reaction with the DLR-III lightweight manipulator arm," in *Proc. IEEE/RSJ Int. Conf. Intelligent Robots and Systems*, 2003, pp. 634–639.
[6] G. Pratt and M. Williamson, "Series elastic actuators," *Proc. IEEE/RSJ Int. Conf. Intelligent Robots and Systems*, vol. 1, p. 399, 1995.
[7] S. Jacobsen, H. Ko, E. Iversen, and C. Davis, "Antagonistic control of a tendon driven manipulator," in *Robotics and Automation, 1989. Proceedings., 1989 IEEE International Conference on*, May 1989, pp. 1334–1339 vol.3.
[8] V. Potkonjak, B. Svetozarevic, K. Jovanovic, and O. Holland, "The puller-follower control of compliant and noncompliant antagonistic tendon drives in robotic systems," *INTERNATIONAL JOURNAL OF ADVANCED ROBOTIC SYSTEMS*, vol. 8, no. 5, pp. 143–155, 2011.
[9] P. Tomei, "A simple PD controller for robots with elastic joints," *IEEE Trans. Autom. Control*, vol. 36, no. 10, pp. 1208–1213, 1991.
[10] M. W. Spong, "Modeling and control of elastic joint robots," *J. Dynamic Systems, Measurement, and Control*, vol. 109, no. 4, pp. 310–318, 1987.
[11] A. De Luca and P. Lucibello, "A general algorithm for dynamic feedback linearization of robots with elastic joints," in *Robotics and Automation, 1998. Proceedings. 1998 IEEE International Conference on*, vol. 1, May 1998, pp. 504–510 vol.1.
[12] A. D. Luca, B. Siciliano, and L. Zollo, "PD control with on-line gravity compensation for robots with elastic joints: Theory and experiments," *Automatica*, vol. 41, no. 10, pp. 1809 – 1819, 2005. [Online]. Available: http://www.sciencedirect.com/science/article/pii/S000510980500186X
[13] A. De Luca and W. Book, *Springer Handbook of Robotics*. Springer, 2008, ch. Robots with Flexible Elements, pp. 287–319.
[14] L. L. Tien, A. A. Schäffer, and G. Hirzinger, "Mimo state feedback controller for a flexible joint robot with strong joint coupling," in *Proc. IEEE Int. Conf. Robotics and Automation*, 2007.
[15] C. Ott, A. Albu-Schaffer, A. Kugi, and G. Hirzinger, "On the passivity-based impedance control of flexible joint robots," *Robotics, IEEE Transactions on*, vol. 24, no. 2, pp. 416–429, April 2008.
[16] M. Zinn, B. Roth, O. Khatib, and J. K. Salisbury, "A new actuation approach for human friendly robot design," in *Proc. IEEE Int. Conf. Robotics and Automation*, 2004, pp. 249–254.
[17] M. Vukobratovic, D. Surdilovic, Y. Ekalo, and D. Katic, *Control of Robots in Contact Tasks: A Survey*. World Scientific, 2009, ch. 1, pp. 1–76. [Online]. Available: http://www.worldscientific.com/doi/abs/10.1142/9789812834768_0001
[18] R. Van Ham, T. Sugar, B. Vanderborght, K. Hollander, and D. Lefeber, "Compliant actuator designs," *IEEE Robot. Autom. Mag.*, vol. 16, no. 3, pp. 81–94, 2009.
[19] T. Lens, J. Kunz, and O. von Stryk, "Dynamic modeling of the 4 DoF BioRob series elastic robot arm for simulation and control," in *Simulation, Modeling, and Programming for Autonomous Robots*, ser. Lecture Notes in Artificial Intelligence. Springer, 2010, pp. 411–422.
[20] T. Lens and O. von Stryk, "Design and dynamics model of a lightweight series elastic tendon-driven robot arm," in *Proc. IEEE Int. Conf. on Robotics and Automation (ICRA)*, Karlsruhe, Germany, May 6-10 2013, pp. 4512 – 4518.
[21] T. Lens, J. Kirchhoff, and O. von Stryk, "Dynamic modeling of elastic tendon actuators with tendon slackening," in *IEEE-RAS Int. Conf. Humanoid Robots*, 2012, pp. 779–784.
[22] J. G. Ziegler and N. B. Nichols, "Optimum Settings for Automatic Controllers," *Transactions of ASME*, vol. 64, pp. 759–768, 1942.

Copyright (c) 2016 IEEE. Personal use of this material is permitted. Permission from IEEE must be obtained for all other uses, in any current or future media, including reprinting/republishing this material for advertising or promotional purposes, creating new collective works, for resale or redistribution to servers or lists, or reuse of any copyrighted component of this work in other works.